Coupled modes in plano-convex bulk acoustic wave quartz plates resonators

24th European Frequency and Time Forum
13-16 April 2010

J.Imbaud, B.Dulmet, R.Bourquin

Time and Frequency Dept., FEMTO-ST, CNRS, ENSMM, UFC, UTBM, Besançon, France
joel.Imbaud@ens2m.fr

INTRODUCTION

The usual analytical models of plano-convex resonators, in particular the asymptotic model of Stevens and Tiersten [1], give the description of the trapped modes, i.e. modes which are confined in the center of the resonator. They are "one mode" models, *i.e.* they assume that, in practice, only one mode essentially contributes to the electrical response in the near vicinity of a resonant frequency, while other modes of vibration existing in the resonator have very small amplitude of vibration and may be neglected.

We have observed by classical X-Ray Lang topography that the main thickness-shear (TS) modes (B or C) of a plano-convex quartz crystal resonator are accompanied by a non-trapped additional vibration, which is extended on the whole surface of the resonator. Its distribution of amplitude exhibits a short periodic behavior in the plane of the resonator. This vibration is observed only in a small frequency range in the vicinity of the resonant frequency, typically the bandwidth of the resonance. It appears that the amplitude of this additional vibration is related to the vibration amplitude of the main mode and that it is not directly driven by the electric field. Thus, this additional vibration appears mechanically driven (or coupled) by the main TS vibration. To support this concept, we give an example of computation of its amplitude in the simple case of a two dimensional AT-Cut resonator. The same procedure can be obviously applied in the general three-dimensional case of a doubly rotated resonator. A flexural vibration accompanying the trapped-energy mode and originated by a defect (additional mass) has already been reported and analyzed in [2]. Another occurrence of coupling (or simultaneous excitation) between thickness shear and flexure was also presented in [3].

X-RAYS TOPOGRAPHIES

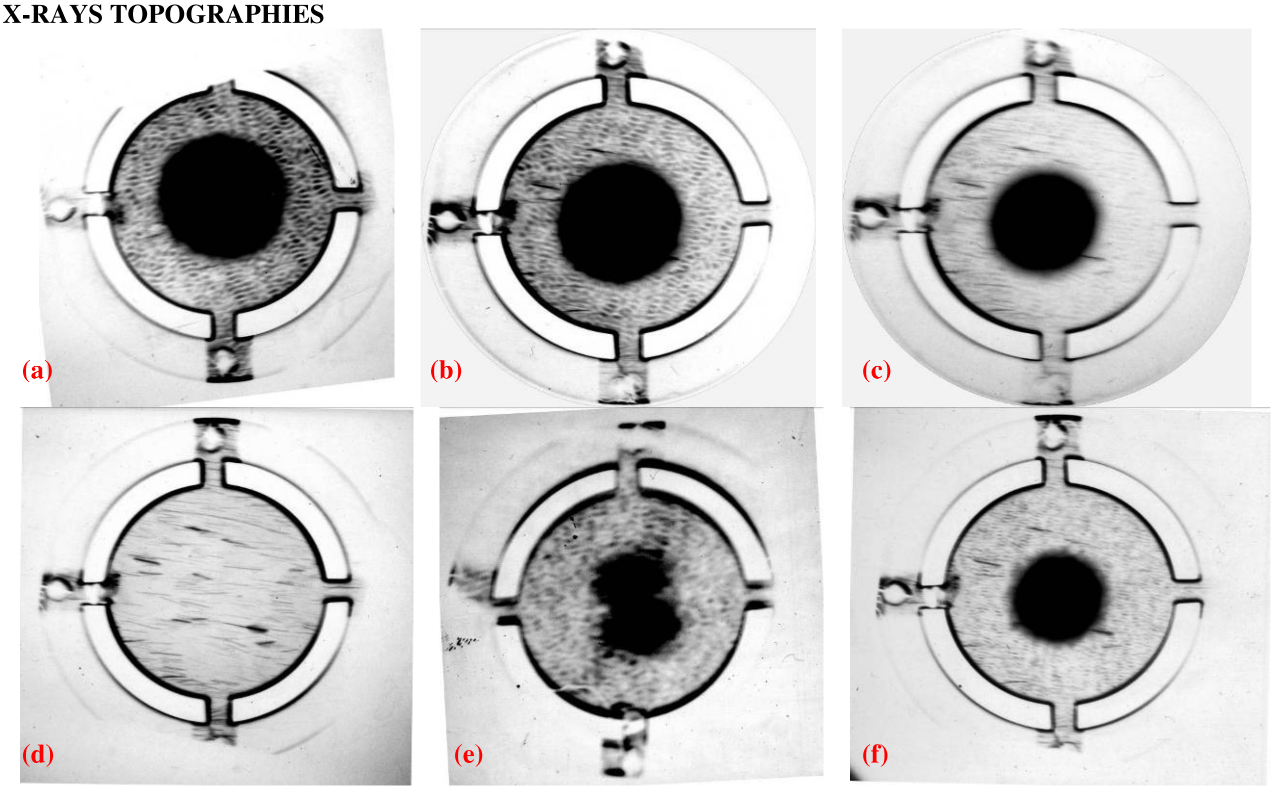

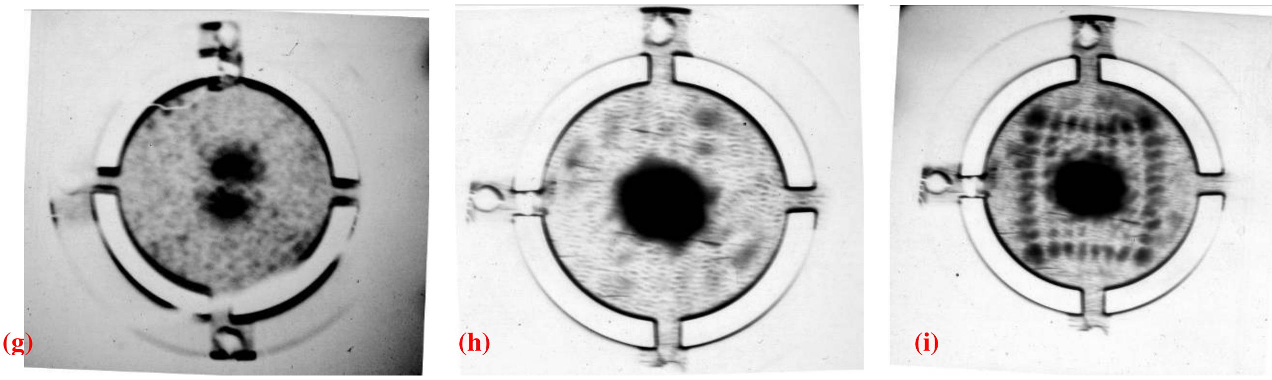

Fig. 1: X-Ray topographies of SC-cut resonator.

X-Rays topographies are obtained using a Lang Camera. The studied plano-convex resonator is of SC-Cut (thickness $2h_0$= 1 mm, radius of curvature R_C=300mm, diameter of central disk = 15mm). All topographies have been performed with the same drive level applied to the resonator. A high drive level is necessary to see the untrapped vibration in the outer part of the resonator. This vibration is not visible at drive level usually used for the topographies. So, on the film, the central region is saturated by the trapped part of the vibration. The synthesizer used to excite the resonator is phase-locked. Two reticular planes have been chosen: the (100) plane to visualize essentially the vibration corresponding to the C-mode, and the $(1\bar{2}2)$ plane to privilege the visualization of the displacement component along the projection of the Z optical axis into the plane of the resonator.

Picture (a) to (c) of figure1 show the topographies of the resonator driven on the 3^{rd} overtone of C-mode (f = 5007 kHz) for three values of phase-shift between the applied voltage and the external current. The reticular plane is (100). It may be observed that the amplitude of the untrapped vibration is lower when the resonator is not excited at its maximum of resonance. The picture (d) shows the same resonator when it is excited at a frequency shifted of 7 kHz far from the resonance. No vibration can be observed. The topography (e) is also for the 3^{rd} overtone of C-mode, but it is obtained by using the $(1\bar{2}2)$ plane. The pattern of the trapped part of the vibration exhibits two areas, in accordance with the interferometric measurement of [4].

The 5^{th} overtone of the C-mode is depicted on the topographies (f) and (g). In accordance with the asymptotic theory of the contoured resonator, the vibration is more confined in the center of the plate and its amplitude is lower than for the 3^{rd} overtone. The amplitude of the untrapped vibration is also lowered.
The picture (h) is for the 3^{rd} overtone of the B-mode, the untrapped vibration is also visible.
The last topography (i) is for the 5^{th} overtone of B-mode. In this case we observe a superposition of two usual trapped modes: the (5,0,0) mode of B-family and a high order anharmonic (5,7,10) of the 5^{th} overtone of the C-mode. In this case, both modes are excited by the electric field. The fact that the (5,7,10) can be excited in such a way is due to a symmetry defect of the resonator.

In counterpart, the untrapped vibration in the other topographies appears to be directly correlated to the vibration of the trapped part.

The wavelength of the untrapped vibration is of the order of 0.3 mm – see picture (a) – *i.e.* it has the same order than the wavelength in the thickness of the resonator. This observation indicates that the “flexure” may play a predominant role.

MODELLING

Two-dimensional model of contoured AT Cut resonator including “flexure" branch

The analysis is based on the dispersion curves [5]. The X-Ray observation shows that one must combine several branches of dispersion curves. To illustrate the mechanism, we consider the simplified case of a two dimensional contoured AT-Cut resonator and we only take into account the coupling between the thickness shear (TS) mode and the flexural wave. To complete this approach, the first requirement is to model the flexure part (seen as the u2 component) of the mode of vibration in a plano-convex resonator.

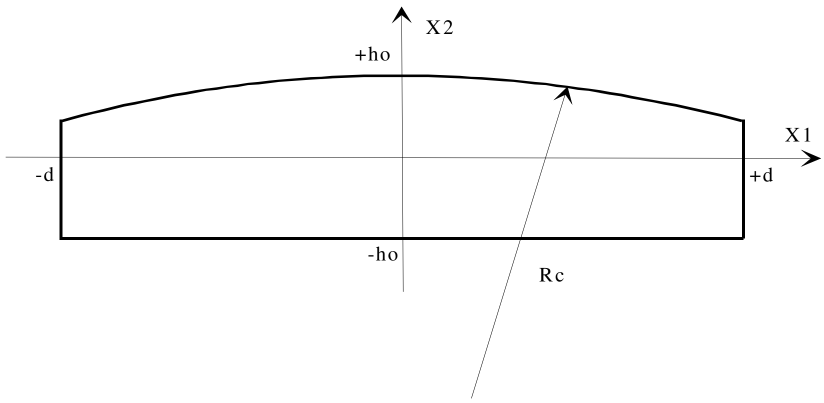

Fig 2: Geometry of resonator.

Basic results for the AT–cut plate

The equations governing the displacement are:

$$\begin{cases} c_{11}u_{1,11} + (c_{12} + c_{66})u_{2,12} + c_{66}u_{1,22} = -\rho\omega^2 u_1 \\ c_{66}u_{2,11} + (c_{12} + c_{66})u_{1,12} + c_{22}u_{2,22} = -\rho\omega^2 u_2 \end{cases} \quad (1)$$

to be associated with the boundaries conditions:

$$T_6 = c_{66}(u_{1,2} + u_{2,1}) = 0 \quad ; \quad T_2 = c_{12}u_{1,1} + c_{22}u_{2,2} = 0 \quad ; \quad x_2 = \pm h_0 \quad (2)$$

The dispersion curves are obtained from the basic set of solutions:

$$\begin{cases} u_1 = [A_1 \sin(\eta_1 x_2) + A_2 \sin(\eta_2 x_2)]e^{-j\xi x_1} e^{j\omega t} \\ u_2 = [B_1 \cos(\eta_1 x_2) + B_2 \cos(\eta_2 x_2)e^{-j\xi x_1} e^{j\omega t} \end{cases} \quad (3)$$

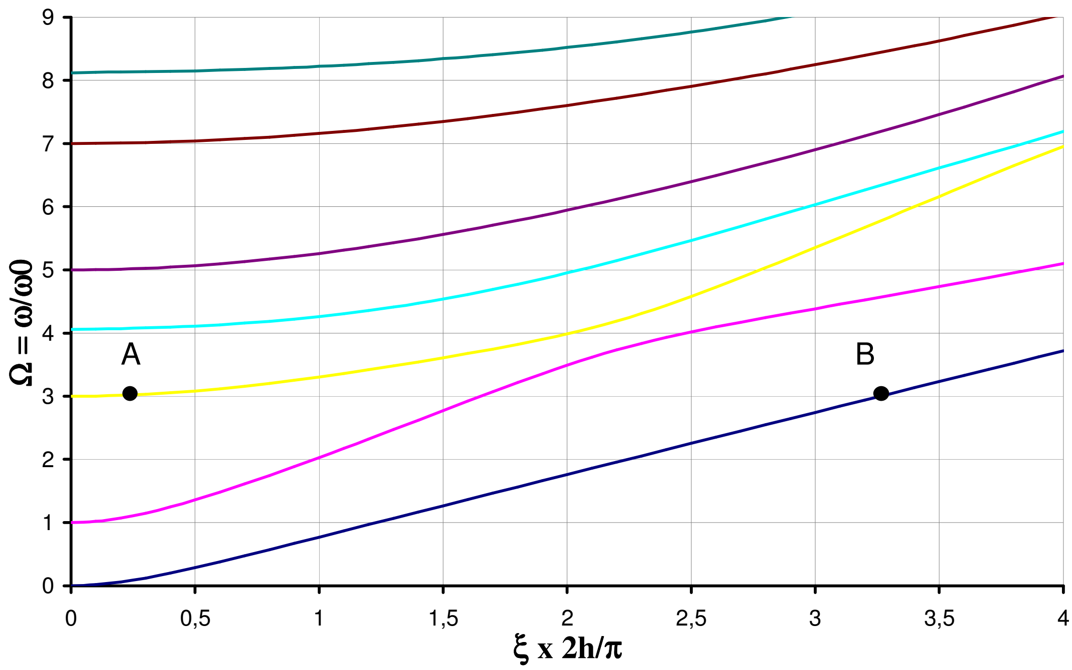

Fig. 3: Dispersion curves for AT-cut.

The dispersion curves are plotted on the figure 3, presenting the dispersion in terms of the reduced frequency $\Omega = \frac{\omega}{\omega_0}$,

where $\omega_0 = \frac{\pi}{2h_0}\sqrt{\frac{c_{66}}{\rho}}$, and $\overline{\xi} = \xi\frac{2h}{\pi}$.

In the vicinity ($\overline{\xi}$ <<1 point A) of the pure thickness-shear (3rd overtone), the components of the displacement are:

$$\begin{cases} u^t{}_1 = A\sin(\eta_1 x_2)e^{-j\xi x_1}e^{j\omega t} \\ u^t{}_2 = B\,[\cos(\eta_1 x_2) + k\cos(\eta_2 x_2)]e^{-j\xi x_1}e^{j\omega t} \\ \eta_1 \cong 3\frac{\pi}{2h} \quad \eta 2 \cong 1.476\frac{\pi}{2h} \quad k \cong -2.3 \end{cases} \tag{4}$$

For a decay number near $\overline{\xi}$ =3 (point B), the displacement of the lowest branch (the so-called "flexure" branch because at small decay number $\overline{\xi}$ the motion tends to the flexure, at high $\overline{\xi}$ it is a mixing of flexure and shear strain) is:

$$\begin{cases} u^f{}_1 = [A_1\sin(\eta_1 x_2) + A_2\sin(\eta_2 x_2)]e^{-j\xi x_1}e^{j\omega t} \\ u^f{}_2 = [B_1\cos(\eta_1 x_2) + B_2\cos(\eta_2 x_2)e^{-j\xi x_1}e^{j\omega t} \\ \eta_1 \cong 0.66\frac{\pi}{2h} \quad \eta 2 \cong 3.94\frac{\pi}{2h} \\ A_1 \cong -1.08 \quad A2 \cong -0.48 \quad B_1 \cong 0.97 \quad B2 \cong 1.09 \end{cases} \tag{5}$$

Contoured resonator

The known dispersion relation [1] describes the asymptotic behavior of thickness–shear branch of the dispersion curves at small values of the lateral wavenumber ξ:

$$M_n\xi^2 + (n^2\pi^2 / 4h^2)c_{66} = \rho\omega^2 \tag{6}$$

From this relation, we deduce the differential equation governing the mode shape:

$$M_n\frac{\partial^2 u}{\partial x_1^2} - \frac{n^2\pi^2 c_{66}}{4h_0^2}(1 + \frac{x_1^2}{2R_c h_0})u + \rho\omega^2 u = 0 \tag{7}$$

Since these last results are obtained from the problem defined by (1) and (2), they are valid for both displacement components u_1 and u_2.

The resonant the frequency is given by:

$$\omega_{nm}^2 = \frac{n^2\pi^2 C_{66}}{4h^2\rho}\left[1 + \frac{1}{n\pi}(2m+1)\sqrt{\frac{M_n}{c_{66}}}\right] \tag{8}$$

M_n is the dispersion constant [1] ($M_3 = 76.10^9\,MPa$), and the main displacement has the form:

$$\begin{aligned} u^t{}_1 &= U\sin\left(\frac{n\pi x_2}{2h}\right)H_m\left(\sqrt{\alpha_n}x_1\right)e^{-\alpha_n\frac{x_1^2}{2}} \\ \alpha_n &= n\pi\sqrt{\frac{c_{66}}{8R_c h_0^3 M_n}} \end{aligned} \tag{9}$$

where $H_m(x_1)$ is the Hermite Polynomial [6].

Determination of displacement $u^t{}_2$ accompanying $u^t{}_1$:

$u^t{}_2$ is obtained by substituting above solution(4) in (1.1) as second member:

$$c_{66}u^t{}_{2,11} + c_{22}u^t{}_{2,22} + \rho\omega^2 u^t{}_2 = (c_{12} + c_{66})\eta_1\alpha_3 x_1 \cos(\eta_1 x_2)\ e^{-\alpha_n \frac{x_1^2}{2}} \tag{10}$$

Using Green's formalism [7], one obtains:

$$u^t{}_2 = C_1 \bar{u}^t{}_2$$

$$\bar{u}^t{}_2 = N\left[-\cos(\eta_1 x_2) + k\cos(\eta_2 x_2)\right] x_1 \sqrt{2\alpha_3}\, e^{-\frac{\alpha_3 x_1^2}{2}} \tag{11}$$

where $\bar{u}^t{}_2$ is the normalized eigenfunction and :

$$C_1 = \frac{(c_{12} + c_{66})\eta_1 \alpha_3}{\rho\left(\omega_{30}^2 - \omega_{31}^2\right)} \int_{-h}^{+h}\int_{-\infty}^{+\infty} \bar{u}^t{}_2 x_1 \cos(\eta_1 x_2)\, e^{-\alpha_n \frac{x_1^2}{2}} dx_1 dx_2 \tag{12}$$

For a 5 MHz resonator operating on the 3rd overtone ($2h_0$=0.997 mm, R_c =150 mm, $N = 0.4073 \dfrac{\alpha_3^{1/4}}{h^{1/2}}$), the $u^t{}_1$ (green curve) and the $u^t 2$ displacements (red curve) [for clarity the displacement: u_1 is divided by 10 on the graph] of the mode shape are:

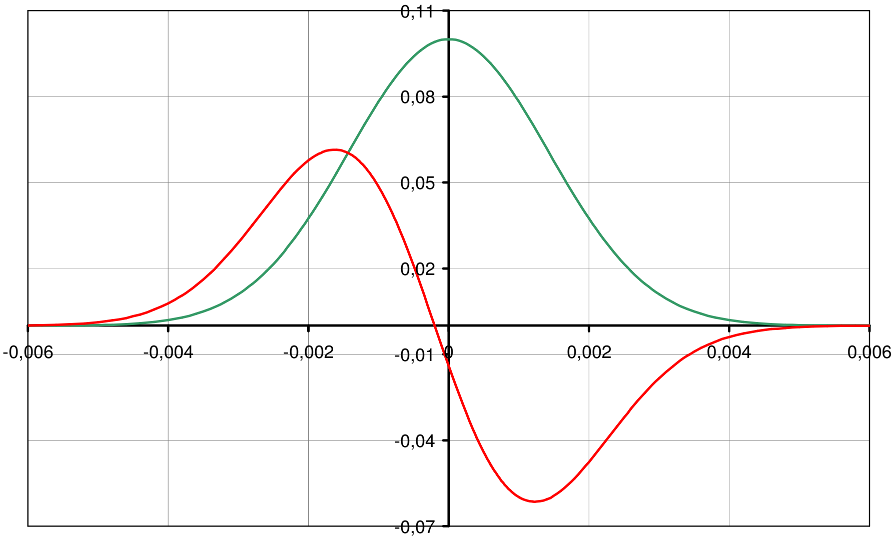

Fig.4: Displacements of thickness shear and flexure at the surface of a contoured resonator.

Calculus of u1 and u2 for the untrapped part of the vibration

We consider again the equations (1) in which the displacements are the sum of the $(u^f{}_i)$ part coming from the unknown flexure and the $(u^t{}_i)$ part coming from the known thickness shear acting as a driving term. We assume that, in the thickness shear branch, the partial derivatives of displacement with respect to x_1 are of one order of magnitude smaller than its derivatives with respect to x_2. Also, $u^t{}_2$ is expected to be one order of magnitude smaller than $u^t{}_1$, while $c_{22} > c_{12} + c_{66}$. Accordingly, we use the following system to simply describe the coupling of flexure with thickness-shear:

$$\begin{cases} c_{11}u^f{}_{1,11} + (c_{12} + c_{66})u^f{}_{2,12} + c_{66}u^f{}_{1,22} + \rho\omega^2 u^f{}_1 = c_{66}u^t{}_{1,22} \\ c_{66}u^f{}_{2,11} + (c_{12} + c_{66})u^f{}_{1,12} + c_{22}u^f{}_{2,22} + \rho\omega^2 u^f{}_2 = c_{22}u^t{}_{2,22} \end{cases} \tag{13}$$

with :

$$\begin{cases} u^{f(m)}{}_1 = [A_1 \sin(\eta_1 x_2) + A_2 \sin(\eta_2 x_2)]\Big|\begin{matrix}\cos\\ \sin\end{matrix}(\xi_m\, x_1) \\ u^{f(m)}{}_2 = [B_1 \cos(\eta_1 x_2) + B_2 \cos(\eta_2 x_2)]\Big|\begin{matrix}\cos\\ \sin\end{matrix}(\xi_m\, x_1) \end{cases} \tag{14}$$

If $\bar{u}^{f(m)}$ is the m^th^ normalized eigenfunction:

$$\int_{-h}^{+h}\int_{-d}^{+d}\left[\left(\bar{u}^{f(m)}{}_1\right)^2 + \left(\bar{u}^{f(m)}{}_2\right)^2\right]dx_1 dx_2 = 1 \tag{15}$$

the solution of (13) can be expressed as the sum:

$$u^f{}_i = \sum_m C_m \bar{u}^{f(m)}{}_i \tag{16}$$

where C_m is given by :

$$\rho(\omega_{30}{}^2 - \omega^{(f)}{}_m{}^2)C_m = \int_{-h}^{+h}\int_{-\infty}^{+\infty}\left(c_{66} u^t{}_{1,22}\bar{u}^{f(m)}{}_i + c_{22} u^t{}_{2,22}\bar{u}^{f(m)}{}_i\right)dx_1 dx_2 = I_1 + I_2 \tag{17}$$

Let us substitute the values (5) for η_1 and η_1 in (14). Since the x_2 – dependence of $u^f{}_1$ and $u^f{}_2$ can be either in sinus or cosinus, the resonant frequencies $\omega^{(f)}{}_m$ can be approximately determined from the values of ξ_m that minimize the integral:

$$\left\langle T^2 \right\rangle = \int_{-h}^{+h}\left(T_1^2 + T_6{}^2\right) dx_2 \ \text{ at } \ x_1 = \mp d \tag{18}$$

The expression of $\omega^{(f)}{}_m = \Omega\,\omega_0$ in terms of ξ near the pure thickness resonance is provided by the following approximation of the "flexure" branch near the B point: $\Omega \approx -0.185 + 0.978\dfrac{2h}{\pi}\xi$.

For a resonator with a width $d = 8h$, the normalizing factor of $u^{f(m)}$ is $\approx 0.23/h$. The integrals I1 and I2 in (17) decrease rapidly when ξ increases (Table 1):

Table 1

$\xi\pi/2h$	0.5	1	2
I1	0.55	2.9 10^{-4}	2.4 10^{-17}
I2	-0.52	-5.5 10^{-4}	-9 10^{-17}

C_m depends directly on the difference: $\omega_{30} - \omega^{(f)}{}_m$ between the frequencies. It means that C_m is strongly dependant of the width of the resonator. One must also keep in mind that, since the additional vibration is not trapped, it is damped and the frequency $\omega^{(f)}{}_m$ must be considered complex.

CONCLUSION

For a perfectly symmetric resonator, the amplitude of the flexure accompanying the thickness shear mode is very small if the resonator has a large diameter.
In practice a lack of symmetry will increase the contribution of the flexural wave branch. For resonators operating in overtone modes (n>1), the contribution of the lower thickness shear branch must be also taking into account.

REFERENCES

[1] D.S. Stevens, H.F. Tiersten, "An analysis of doubly rotated quartz resonators utilizing essentially thickness modes with transverse varation", J.A.S.A., Vol. 79, No. 6, pp. 1811-1826, June 1986.
[2] E.P. EerNisse, E. Benes, M. Schmid, "The role of localized rotational imbalance in drive level dependence phenomena", Proc. of the 2002 Int. Freq. Cont. Symp., pp. 2-7.

[3] W.J. Spencer, in Physical Acoustics, Vol. 5, Part A, Acad. Press, New York, 1968, pp.127-161.
[4] Takehiko Adachi, Masumi Okazaki, Yasuo Tsuzuki, “Improvements of Laser Interferometric Measurement System of Vibration Displacement”, Proc. of the 37th Ann. Freq. Cont. Symp., 1983, pp. 187-193.
[5] H.F. Tiersten, “Linear Piezoelectric Plate Vibrations”, Plenum Press, New York, 1969.
[6] M. Abramowitz, I.A. Stegun ed., “Handbook of Mathematical Functions”, Dover Publications, New York, 1972.
[7] J. Mathews, R.L. Walker, “Mathematical Methods of Physics”, Addison-Wesley, Redwood City, 1970.